ARTICLE

In Situ Fabrication of *meso*-Tetrakis(4-sulfonatophenyl)porphyrin Nanostructures with Excitonic Absorption on Glass Substrate

Palanisamy Kalimuthu[†] and S. Abraham John*

Department of Chemistry, Gandhigram Rural University, Gandhigram, Dindigul, Tamilnadu, India-624 302

ABSTRACT In this article, we report in situ fabrication of *meso*-tetrakis(4-sulfonatophenyl)porphyrin (TPPS) nanostructures with excitonic absorption on glass substrate. The exposure of TPPS thin film coated on a glass plate to HCl vapor resulted in the formation of nanostructures of TPPS. The formed TPPS nanostructures on glass plate were characterized by UV−vis, steady state emission spectral techniques, atomic force microscopy, and high resolution transmission electron microscopy (HR-TEM). A new sharp and intense absorption band (excitonic band) at 490 nm was observed for TPPS nanostructures on glass plate. Protonation of tertiary nitrogen atoms of TPPS ring by HCl molecules leads to the formation of nanostructures of J-aggregates of TPPS on glass surface. The height of the TPPS nanostructures was found to be 50−170 nm with an average width of 100 nm. HR-TEM images showed that the formed TPPS J-aggregates consist of tiny nanorods. The size of the nanostructures was tuned successfully by varying the concentration of TPPS used for thin film preparation.

KEYWORDS: *meso*-tetrakis(4-sulfonatophenyl)porphyrin • in situ fabrication • porphyrin nanostructures • J-aggregate • excitonic absorption • hydrogen chloride vapor

1. INTRODUCTION

Porphyrin nanostructures attracted researchers in recent years because of their applications in various fields including molecular electronics and photovoltaics (1−3). Supramolecular structure by means of self-assembly of porphyrin molecules facilitates to mimic the natural phenomenon such as photosynthesis (4). In natural photosynthetic systems, the tetrapyrrole derivative, chlorophyll, is often self-organized into nanoscale superstructures that perform many of the essential light-harvesting and excited state energy and electron transfer functions (5−8). The light-harvesting rods of the chlorosomes of green-sulfur bacteria are composed entirely of aggregated bacteriochlorophyll (5−8). Aggregates which exhibit a red shift with respect to the monomer absorption band are termed as J-aggregates, and those which have a blue shift are referred as H-aggregates (9). Dye molecules are self-assembled with dipole−dipole interaction in J-aggregates with a "head-to-tail" manner while in H-aggregates they have a "face-to-face" manner (9, 10). The synthetic compound, *meso*-tetrakis(4-sulfonatophenyl)porphyrin (TPPS) has been the most studied compound for J-aggregate formation since it forms J-aggregates simply under acidic conditions and also in the presence of alkaline earth metal ions, monoamines, surfactants, and cationic porphyrins (11−17). The morphology and internal structure of TPPS J-aggregates were studied in detail by various researchers (3, 4, 6, 11, 12, 18). It was proposed that the TPPS molecules were stacked in head-to-tail fashion in linear arrays. These arrays are placed together in a parallel manner in a nanorod (3, 6, 18). In some cases, several tiny nanorods compile to form a bundle of nanorods (3, 6, 18). For practical applications, the formation of nanostructured TPPS aggregates on solid substrates is more attractive because it can be useful for the fabrication of organic solar cells (19), nonlinear optical materials (20), sensors (21), and light mediated charge storage devices (22, 23). To date, few reports have been published for J- and H-aggregates of water-soluble TPPS on solid substrates by layer-by-layer assembly (11, 24, 25) and casting (18) methods. The structure of the obtained thin film is very important to influence the sensing capability in gas sensors (26). The nanostructured thin film will offer more surface area and, hence, enhancement in the sensitivity toward gases (26). In a recent report, interaction of surface plasmon with an excited molecule using TPPS J-aggregate was studied (27). This study opens a new avenue to understand the photophysical properties of molecules in the excited state. Therefore, it is necessary to obtain pure TPPS J-aggregates without any additives on the surface for such studies. It is also emphasized that the film obtained without any additives is important to increase the sensitivity of the gas sensor devices (26, 28). It is interesting to study the in situ fabrication of nanostructured TPPS J-aggregate on solid surface without any additives like excess mineral acids, amino acids, and ionic liquids. Very recently, we reported the aggregation of water insoluble *meso*-tetramesitylporphy-

* To whom correspondence should be addressed. Telephone: 91-451-2452371. Fax: 91-451-2453071. E-mail: abrajohn@yahoo.co.in.

Received for review August 19, 2010 and accepted October 21, 2010

[†] Current Address: Department of Materials and Applied Chemistry, College of Science and Technology, Nihon University, Tokyo 101-8308.

DOI: 10.1021/am100766b

2010 American Chemical Society

Published on Web 11/02/2010

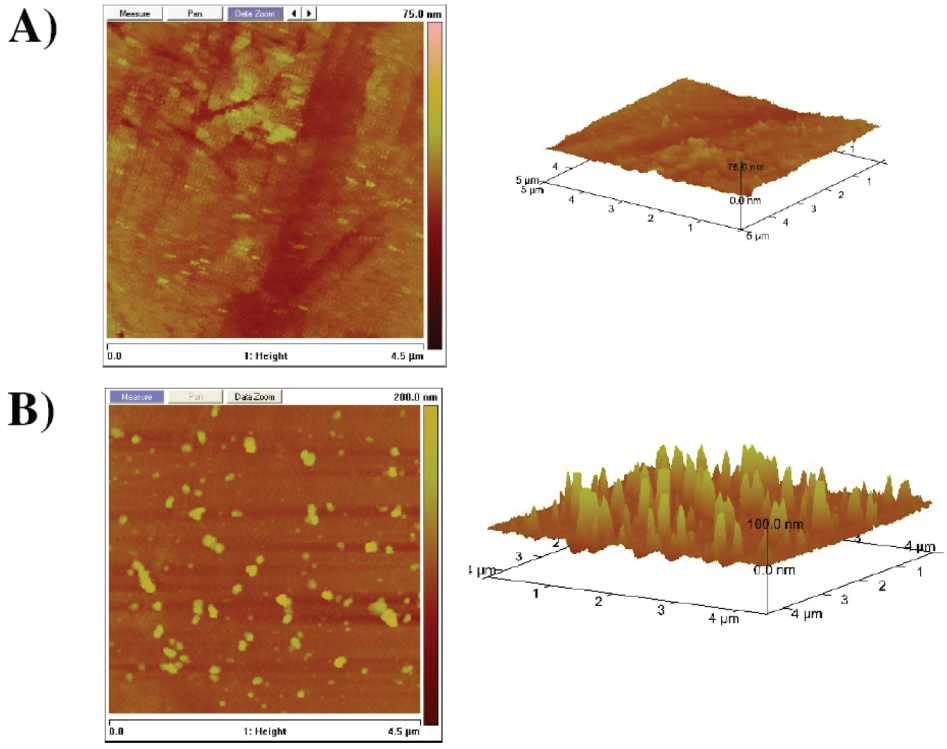

FIGURE 1. Top down and 3D AFM images of (A) TPPS thin film and (B) TPPS thin film after exposed to HCl gas.

rin (MTMP) on solid substrate (29). When compared to TPPS J-aggregates formed in solution, no sharp J-band was observed for the MTMP J-aggregates (18). In this article, we wish to report the in situ fabrication of nanostructures of water-soluble TPPS with excitonic absorption (18) on glass substrate. The formation of nanostructured TPPS aggregates with excitonic absorption was confirmed by spectral, atomic force microscopy (AFM) and high resolution transmission electron microscopy (HR-TEM) techniques. We have successfully adopted our new approach (29) to fabricate the TPPS nanostructures with excitonic absorption in situ without any additives. This may put forward the improvement of the fabrication of photoresponsive nanodevices.

2. EXPERIMENTAL SECTION

TPPS was purchased from Fluka and was used as supplied. UV−vis spectra were recorded using a Perkin-Elmer UV−vis Lambda35 spectrophotometer. Fluorescence spectra were recorded using a Perkin-Elmer LS 55 model fluorimeter. The TPPS J-aggregate was excited at 490 nm for fluorescence measurements. A thin film of TPPS on glass plate was prepared using 0.01 M TPPS in a 9:1 ethanol and water mixture by the spin coating method. A clean glass plate was placed on a rotating plate with 3000 rpm and 0.1 mL of 0.01 M TPPS added dropwise. The TPPS coated plate was dried at room temperature in nitrogen atmosphere. The setup for exposure of TPPS thin film to HCl gas is shown in Supporting Information Figure S1. Standard dry HCl gas (19 ppm) diluted with nitrogen was used for J-aggregate formation. The thin film was exposed to HCl vapor for 1 min and then flushed with nitrogen gas for 30 s to remove excess HCl vapor. AFM images were obtained using the MultiMode V Scanning Probe microscope (SPM) for TPPS coated glass plates before and after exposure to HCl vapor. HR-TEM images were obtained using a JEOL JEM 3010 operating at 200 kV.

3. RESULTS AND DISCUSSION

3.1. Fabrication of Nanostructures of TPPS on Glass Plate. A clean glass plate was coated with TPPS of 10 nm thickness (Figure 1A). To obtain the nanostructures of TPPS, the glass plate containing TPPS thin film was exposed to HCl vapor. Figure 1B shows the AFM image of TPPS thin film after exposure to HCl vapor. One can observe the formed nanosized aggregates on the surface in contrast to TPPS thin film.

The 3D view (Figure 1B) indicates that the nanostructures of TPPS aggregates are grown vertically in contrast to TPPS thin film (18). From Figure 1B, the height of the nanostructures of TPPS was found to be 50−170 nm (also see Supporting Information Figure S2 and Figure S3) with the average width of 100 nm. The close 3D view of Figure 1B reveals that bundles of small nanorods of TPPS are assembled together in a parallel manner to form a bigger sized nanostructure (Figure 2). To confirm the presence of tiny nanorods in the nanostructures of TPPS, HR-TEM images were taken and are shown in Figure 3.

Figure 3A shows the TEM image of TPPS thin film after exposure to HCl vapor. Similar to AFM image as shown in Figure 1A, nanosized aggregates were observed. The magnified view of the top edge of the TPPS nanostructure in Figure 3A reveals the presence of tiny nanorods of TPPS with a size of ∼40 nm. The images obtained from AFM (Figure 2) and TEM (Figure 3) confirm the presence of small sized nanorods are held together in the nanostructures.

3.2. Spectroscopic Investigation of TPPS Nanostructures. The TPPS nanostructures formed on glass substrate were characterized by spectroscopic techniques (1, 3, 10, 30). The absorption spectrum of TPPS thin film on

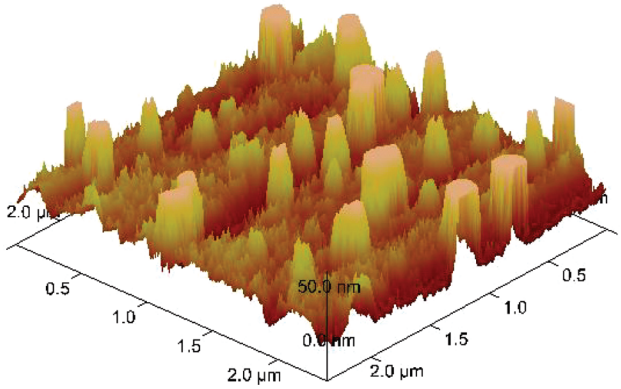

FIGURE 2. Magnified view of nanostructures of TPPS on glass plate.

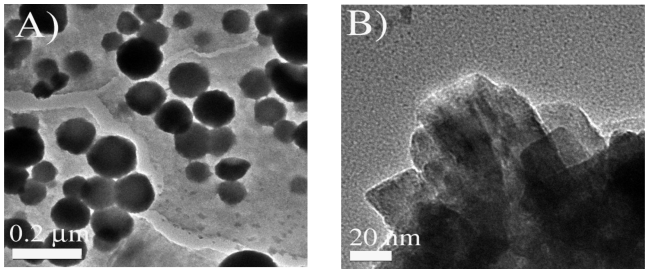

FIGURE 3. HR-TEM images of (A) nanostructures of TPPS (a thin film of TPPS on copper grid exposed to HCl vapor) (B) magnified view of the top edge of one such nanostructure of TPPS.

a glass plate shows a Soret band at 405 nm and Q bands at 520, 559, 606, and 677 nm (Figure 4A curve a). The Soret band was blue-shifted by 8 nm in contrast to TPPS in water (4B curve a) (31). Such behavior may be due to H-aggregates of TPPS in a condensed state on glass substrate (11, 32). When the TPPS thin film was exposed to gaseous HCl, surprisingly, new sharp and intense absorption bands at 490 nm (J- or excitonic band) and 703 nm (Figure 4A curve b), characteristic of TPPS J-aggregates, were observed (1, 3, 10, 30, 33). The observed spectral feature at 490 nm is very similar to TPPS J-aggregates in solution (Figure 4B) (18).

Figure 5 shows the emission spectra of a TPPS thin film before and after exposure to HCl gas. After exposure to HCl vapor, the formed nanostructures have a characteristic emission of TPPS J-aggregate at 728 nm (34). The appearances of excitonic absorption at 490 nm and emission at 728 nm suggest that the formed nanostructures after the exposure of TPPS thin film to HCl vapor are TPPS J-aggregates.

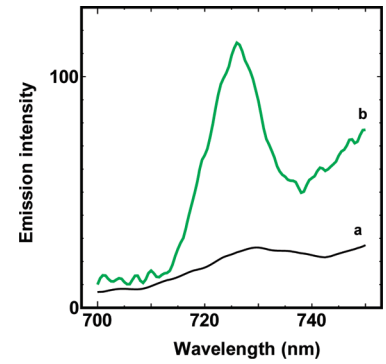

FIGURE 5. Fluorescence spectrum in the region of 700−750 nm of (a) TPPS thin film and (b) TPSS thin film after exposure to HCl vapor.

From the microscopic and spectroscopic evidence, it is proposed that the formation of nanostructured aggregates on the surface is due to the molecules in the TPPS thin film after protonation by HCl vapor moved to form aggregates on glass plate. It has been shown that the porphyrin molecules are mobile on solid surfaces (33, 35). The driving force behind this movement and in situ formation of nanostructured aggregates of TPPS molecules is the appearance of a strong electrostatic attractive force between positively charged tertiary nitrogen atoms in the ring of protonated TPPS molecules and negatively charged peripheral sulfonato groups. When TPPS thin film was exposed to HCl vapor, protonation occurs on the tertiary nitrogen atoms of the TPPS ring similar to protonation in solution phase (1, 3, 10, 32). In our previous report, the nanostructured aggregates of *meso*-tetramesitylporphyrin (MTMP) was formed on the basis of electrostatic interaction between protonated (positively charged) nitrogen atoms of porphyrin and intercalated chloride ions between the MTMP molecules (29), but in the present study, the electrostatic attraction between the protonated nitrogen atoms and peripheral sulfonato groups leads to the formation of nanostructured aggregates. Compared to MTMP (29), this kind of interaction offers the TPPS molecules to slip over each other perfectly as proved by the

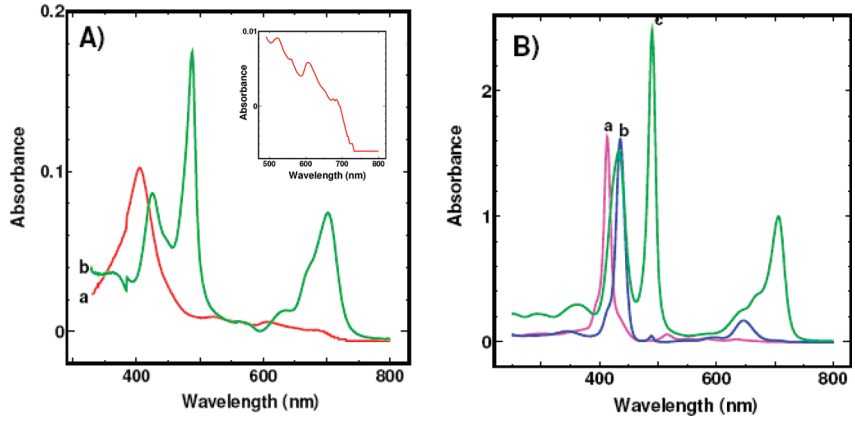

FIGURE 4. (A) Absorption spectra of (a) TPPS thin film on glass plate, (b) TPPS thin film after exposure to gaseous HCl. Inset: Expanded view of Q bands of curve a. (B) Absorption spectra of (a) 10 μM TPPS in water, (b) mixture of equal volumes of 10 μM TPPS and 0.6 M HCl, and (c) 10 μM TPPS with excess HCl.

appearance of the excitonic band at 490 nm in the absorption spectrum (Figure 4A curve b).

Further, we have tuned the size of the nanostructures by changing the concentration of TPPS solution used for the formation of thin film. By lowering the concentration of TPPS solution, the thickness of the thin film was decreased to 3 nm. This thin film forms nanostructures of 20 nm height and 50 nm width (Supporting Information Figure S4) on exposure to HCl vapor. These results indicate that the length and size of the nanostructures were successfully tuned by varying the concentration of TPPS used for the thin film formation.

4. CONCLUSION

In conclusion, we have demonstrated the in situ fabrication of nanostructures of TPPS with an excitonic absorption induced by HCl vapor on solid substrate without any additives. AFM, HR-TEM, and UV−vis and emission spectral techniques confirmed the formation of nanostructures of TPPS on glass substrate. A sharp excitonic or J-band absorption at 490 nm was observed for nanostructures of TPPS J-aggregates formed on solid surface. The height of the formed TPPS nanostructures was found to be 50−170 nm with the average width of 100 nm. The formed TPPS J-aggregates consists of tiny rods of ~40 nm in size. Further, the size of the nanostructure was successfully tuned by varying the concentration of TPPS solution used for the thin film formation.

Acknowledgment. P.K. thanks the University Grants Commission, New Delhi, for the award of Senior Research Fellowship. Financial support from the Defence Research & Development Organization (DRDO; No. No.ERIP/ER/07303675/M/01/1132), New Delhi is gratefully acknowledged.

Note Added after ASAP Publication. This paper was published on the Web on November 2, 2010, with incorrect funding information in the Acknowledgment section. The corrected version was reposted on November 24, 2010.

Supporting Information Available: Experimental details; magnified and additional AFM images. This material is available free of charge via the Internet at http://pubs.acs.org.

REFERENCES AND NOTES

(1) Schwab, A. D.; Smith, D. E.; Bond-Watts, B.; Johnston, D. E.; Hone, J.; Johnson, A. T.; de Paula, J. C.; Smith, W. F. *Nano Lett.* **2004**, *4*, 1261–1265.
(2) Yeats, A. L.; Schwab, A. D.; Massare, B.; Johnston, D. E.; Johnson, A. T.; de Paula, J. C.; Smith, W. F. *J. Phys. Chem. C* **2008**, *112*, 2170–2176.
(3) Schwab, A. D.; Smith, D. E.; Rich, C. S.; Young, E. R.; Smith, W. F.; de Paula, J. C. *J. Phys. Chem. B* **2003**, *107*, 11339–11345.
(4) Vlaming, S. M.; Augulis, R.; Stuart, M. C. A.; Knoester, J.; van Loosdrecht, P. H. M. *J. Phys. Chem. B* **2009**, *113*, 2273–2283.
(5) Staehelin, L. A.; Golecki, J. R.; Fuller, R. C.; Drews, G. *Biophys. J.* **1978**, *85*, 3173–3186.
(6) van Rossum, V. J.; Steensgaard, D. B.; Mulder, F. M.; Boender, G. J.; Schaffner, K.; Holzwarth, A. R.; de Groot, H. J. M. *Biochemistry* **2001**, *40*, 1587–1595.
(7) Olson, J. M. *Photochem. Photobiol.* **1998**, *67*, 61–75.
(8) Blankenship, R. E.; Olson, J. M.; Miller, M. *Antenna Complexes from Green Photosynthetic Bacteria*; Blankenship, R. E.; Madigan, M. T.; Bauer, C. E., Eds.; Kluwer Academic Publishers: Dordrecht, The Netherlands, 1995; pp 339−435.
(9) Eisfeld, A.; Briggs, J. S. *Chem. Phys.* **2006**, *324*, 376–384.
(10) Kubat, P.; Lang, K.; Prochazkova, K.; Anzenbacher, P., Jr. *Langmuir* **2003**, *19*, 422–428.
(11) Kitahama, Y.; Kimura, Y.; Takazawa, K. *Langmuir* **2006**, *22*, 7600–7604.
(12) Egawa, Y.; Hayashida, R.; Anzai, J. *Langmuir* **2007**, *23*, 13146–13150.
(13) Ohno, O.; Kaizu, Y.; Kobayashi, H. *J. Chem. Phys.* **1993**, *99*, 4128–4139.
(14) Ribo, J. M.; Crusats, J.; Farrera, J. A.; Valero, M. L. *J. Chem. Soc., Chem. Commun.* **1994**, *68*, 681–682.
(15) Pasternack, R. F.; Schaefer, K. F.; Hambright, P. *Inorg. Chem.* **1994**, *33*, 2062–2065.
(16) Akins, D. L.; Zhu, H. R.; Guo, C. *J. Phys. Chem.* **1994**, *98*, 3612–3618.
(17) Maiti, N.; Ravikanth, M.; Mazumdar, S.; Periasamy, N. *J. Phys. Chem.* **1995**, *99*, 17192–17197.
(18) Rotomskis, R.; Augulis, R.; Snitka, V. *J. Phys. Chem. B* **2004**, *108*, 2833–2838.
(19) Hasobe, T.; Imahori, H.; Fukuzumi, S.; Kamat, P. V. *J. Mater. Chem.* **2003**, *13*, 2515–2520.
(20) Collini, E.; Ferrante, C.; Bozio, R.; Lodi, A.; Ponterini, G. *J. Mater. Chem.* **2006**, *16*, 1573–1578.
(21) Fujii, Y.; Hasegawa, Y.; Yanagida, S.; Wada, Y. *Chem. Commun.* **2005**, 3065–3067.
(22) Liu, C.; Pan, H.; Fox, M. A.; Bard, A. J. *Chem. Mater.* **1997**, *9*, 1422–1429.
(23) Liu, C.; Pan, H.; Fox, M. A.; Bard, A. J. *Science* **1993**, *261*, 897–899.
(24) Simkiene, I.; Sabataityte, J.; Babonas, G. J.; Reza, A.; Beinoras, J. *Mater. Sci. Eng., C* **2006**, *26*, 1007–1011.
(25) Liu, L.; Li, Y.; Liu, M. *J. Phys. Chem. C* **2008**, *112*, 4861–4866.
(26) Tonezzer, M.; Maggioni, G.; Quaranta, A.; Carturan, S.; Della Mea, G. *Sens. Actuators, B* **2001**, *76*, 42–46.
(27) Salomon, A.; Genet, C.; Ebbesen, T. W. *Angew. Chem., Int. Ed.* **2009**, *48*, 8748–8751.
(28) Tonezzer, M.; Quaranta, A.; Maggioni, G.; Carturan, S.; Della Mea, G. *Sens. Actuators, B* **2007**, *122*, 620–626.
(29) Kalimuthu, P.; John, S. A. *Langmuir* **2009**, *25*, 12414–12418.
(30) Koti, A. S. R.; Periasamy, N. *Chem. Mater.* **2003**, *15*, 369–371.
(31) Castriciano, M. A.; Romeo, A.; Villari, V.; Micali, N.; Scolaro, L. M. *J. Phys. Chem. B* **2003**, *107*, 8765–8771.
(32) Kubat, P.; Lang, K.; Prochazkova, K.; Anzenbacher, Jr., P. *Langmuir* **2003**, *19*, 422–428.
(33) Yokoyama, T.; Yokoyama, S.; Kamikado, T.; Okuno, Y.; Mashiko, S. *Nature* **2001**, *413*, 619–621.
(34) Maiti, N. C.; Mazumdar, S.; Periasamy, N. *J. Phys. Chem. B* **1998**, *102*, 1528–1538.
(35) Grill, L.; Dyer, M.; Lafferentz, L.; Persson, M.; Peters, M. V.; Hecht, S. *Nature Nanotechnol.* **2007**, *2*, 687–691.

AM100766B